

AD A103523

14

NSWC/TR-81-145

LEVEL 17

12

FREE ELECTRON LASER INSTABILITY
FOR A RELATIVISTIC SOLID ELECTRON BEAM
IN A HELICAL WIGGLER FIELD.

BY HAN S. UHM RONALD C. DAVIDSON
AND SCIENCE APPLICATIONS, INC.

RESEARCH AND TECHNOLOGY DEPARTMENT

11

JAN 1981

12 43

15

ARPA Order-3718

9 Final rept.

Approved for public release, distribution unlimited.

DTIC
ELECTE
SEP 1 1981
A



NAVAL SURFACE WEAPONS CENTER

Dahlgren, Virginia 22448 • Silver Spring, Maryland 20910

DTIC FILE COPY

81 8

31 243

411563

mt

UNCLASSIFIED

SECURITY CLASSIFICATION OF THIS PAGE (When Data Entered)

REPORT DOCUMENTATION PAGE		READ INSTRUCTIONS BEFORE COMPLETING FORM
1. REPORT NUMBER NSWC TR 81-145	2. GOVT ACCESSION NO. AD-A103522	3. RECIPIENT'S CATALOG NUMBER
4. TITLE (and Subtitle) FREE ELECTRON LASER INSTABILITY FOR A RELATIVISTIC SOLID ELECTRON BEAM IN A HELICAL WIGGLER FIELD		5. TYPE OF REPORT & PERIOD COVERED Final - Jan 1981
		6. PERFORMING ORG. REPORT NUMBER
7. AUTHOR(s) Han S. Uhm, Ronald C. Davidson, and Science Applications, Inc.		8. CONTRACT OR GRANT NUMBER(s)
9. PERFORMING ORGANIZATION NAME AND ADDRESS Naval Surface Weapons Center Code R41 White Oak, Silver Spring, Maryland 20910		10. PROGRAM ELEMENT, PROJECT, TASK AREA & WORK UNIT NUMBERS 0;
11. CONTROLLING OFFICE NAME AND ADDRESS		12. REPORT DATE January 1981
		13. NUMBER OF PAGES 43
14. MONITORING AGENCY NAME & ADDRESS (if different from Controlling Office)		15. SECURITY CLASS. (of this report) UNCLASSIFIED
		15a. DECLASSIFICATION/DOWNGRADING SCHEDULE
16. DISTRIBUTION STATEMENT (of this Report) Approved for public release, distribution unlimited.		
17. DISTRIBUTION STATEMENT (of the abstract entered in Block 20, if different from Report)		
18. SUPPLEMENTARY NOTES		
19. KEY WORDS (Continue on reverse side if necessary and identify by block number) Free Electron Laser Microwave Emission Relativistic Electron Beam Helical Wiggler Field		
20. ABSTRACT (Continue on reverse side if necessary and identify by block number) The free electron laser instability for a solid relativistic electron beam propagating in combined transverse helical wiggler and uniform axial guide fields is investigated within the framework of the linearized Vlasov-Maxwell equations. It is assumed that $v/\gamma_b \ll 1$, where v is Budker's parameter and $\gamma_b mc^2$ is the electron energy. Stability properties are investigated for the choice of equilibrium distribution function in which all electrons have the same value of the linear combination of transverse and helical invariants,		

DD FORM 1 JAN 73 1473

EDITION OF 1 NOV 65 IS OBSOLETE
S/N 0102-014-6601

UNCLASSIFIED

SECURITY CLASSIFICATION OF THIS PAGE (When Data Entered)

UNCLASSIFIED

SECURITY CLASSIFICATION OF THIS PAGE(When Data Entered)

20. $C_{\perp} - 2\gamma_b m \omega_b C_{\parallel} = \text{const.}$, and a Lorentzian distribution in the axial invariant C_{\parallel} . (Here ω_b is a constant.) The instability growth rate is calculated including a determination of the optimum value of the ratio of beam radius to conducting wall radius (R_0/R_c) for maximum growth. It is found that the maximum growth rate for a solid electron beam is comparable to that for a hollow beam with similar parameters. Moreover, the introduction of a small axial momentum spread ($\Delta/\gamma_b mc \sim$ a few percent) significantly reduces the instability growth rate.

UNCLASSIFIED

SECURITY CLASSIFICATION OF THIS PAGE(When Data Entered)

FOREWORD

The free electron laser instability for a solid relativistic electron beam propagating in combined transverse helical wiggler and uniform axial guide fields is investigated within the framework of the linearized Vlasov-Maxwell equations. It is assumed that $v/\gamma_b \ll 1$, where v is Budker's parameter and $\gamma_b mc^2$ is the electron energy. Stability properties are investigated for the choice of equilibrium distribution function in which all electrons have the same value of the linear combination of transverse and helical invariants. $C_1 - 2\gamma_b m \omega_b C_h = \text{const.}$, and a Lorentzian distribution in the axial invariant C_z . (Here ω_b is a constant.) The instability growth rate is calculated including a determination of the optimum value of the ratio of beam radius to conducting wall radius (R_0/R_c) for maximum growth. It is found that the maximum growth rate for a solid electron beam is comparable to that for a hollow beam with similar parameters. Moreover, the introduction of a small axial momentum spread ($\Delta/\gamma_b mc \approx$ a few percent) significantly reduces the instability growth rate. This research was supported in part by Defense Advance Research Project Agency (DOD) under ARPA Order No. 3718, Amendment No. 12, in part by the Independent Research Fund at the Naval Surface Weapons Center, and in part by the Office of Naval Research.

H. R. Riedl
 H. R. RIEDL
 By direction

Accession For	
NTIS GRA&I	<input checked="" type="checkbox"/>
DTIC TAB	<input type="checkbox"/>
Unannounced	<input type="checkbox"/>
Justification	
By	
Distribution/	
Availability Codes	
Dist	Avail and/or Special
A	

CONTENTS

<u>Chapter</u>		<u>Page</u>
I	INTRODUCTION	7
II	EQUILIBRIUM THEORY AND BASIC ASSUMPTIONS	11
III	LINEARIZED VLASOV-MAXWELL EQUATIONS FOR A TENUOUS BEAM	15
IV	FREE ELECTRON LASER STABILITY PROPERTIES	23
V	CONCLUSIONS	31
	ACKNOWLEDGEMENTS	31
	BIBLIOGRAPHY	39
	APPENDIX A - LONGITUDINAL PERTURBATIONS FOR THE FREE ELECTRON LASER INSTABILITY	A-1

ILLUSTRATIONS

<u>Figures</u>		<u>Page</u>
1 (a&b)	PLOTS OF $G_{\ell s'}(x)$ VERSUS x [EQ. (59)] FOR (a) $\beta_{\ell, s'} = \beta_{0,1}$ AND (b) $\beta_{\ell, s'} = \beta_{1,3}$	33
2	PLOTS OF (a) $x_{\ell s'}$ AND (b) THE CORRESPONDING $G_{\ell s'}^{\phi} = G_{\ell s'}(x_{\ell s'})$ FOR SEVERAL VALUES OF AZIMUTHAL AND RADIAL MODE NUMBERS, ℓ AND s'	35
3	PLOTS OF (a) $Q_{\ell s s'}^E / G_{\ell s'}$ AND (b) $Q_{\ell s s'}^M / G_{\ell s'}$ [EQS. (58) AND (64)] FOR SEVERAL VALUES OF ℓ AND s	36
4 (a&b)	PLOTS OF NORMALIZED GROWTH RATE Ω_i VERSUS $(k + nk_0)/k_0$ FOR $(\ell, s, s') = (3, 2, 1)$, $\gamma_b = 10$, $\nu/\gamma_b = 0.02$, and $\Lambda^2 = 0.01$, WITH (a) $R_0/R_c = x_{31}/\alpha_{4,2}$ FOR THE TE MODE AND (b) $R_0/R_c = x_{31}/\beta_{4,2}$ FOR THE TM MODE.	37

1. INTRODUCTION

In recent years, the free electron laser instability¹⁻⁹ has been extensively investigated with particular emphasis on applications to intense microwave generation. For the most part, previous theoretical analyses of this instability have been carried out either for uniform density beams³⁻⁶ with infinite transverse dimension, or for annular electron beams.^{7,8} The present paper examines the influence of finite radial geometry on the free electron laser instability for a solid electron beam propagating in combined transverse helical wiggler and uniform axial guide fields. The analysis is carried out within the framework of the linearized Vlasov-Maxwell equations, including a determination of the optimum value of beam radius R_0 for maximum growth rate.

The present analysis is carried out for an infinitely long relativistic electron beam propagating in the combined transverse wiggler and uniform axial guide fields described by Eq. (1). Equilibrium and stability properties are calculated for the specific choice of electron distribution function [Eq. (5)],

$$f_b^0 = \frac{n_0}{\pi} \delta(C_1 - 2\gamma_b m \omega_b C_h - 2\gamma_b m \hat{T}_1) G(C_2) ,$$

where n_0 , ω_b , γ_b , and \hat{T}_1 are positive constants, C_1 , C_h , and C_2 are the transverse, helical, and axial invariants¹⁰ defined in Eqs.

(6) - (8), and the axial distribution function is normalized according to $\int_{-\infty}^{\infty} dC_2 G(C_2) = 1$. Equilibrium properties are investigated in Sec. II, and stability properties are examined in Secs. III and IV, assuming that $v/\gamma_b \ll 1$, where v is Budker's parameter, $\gamma_b mc^2$ is the characteristic electron energy, and m is the electron rest mass.

In Sec. III, making use of the linearized Vlasov-Maxwell equations, we obtain the coupled eigenvalue equations (33), (37), (40), (45), and (46) that describe free electron laser stability properties in circumstances where the perturbed transverse fields can be approximated by the vacuum waveguide fields. For short wavelength perturbations, the axial component of the perturbed longitudinal field can be approximated by [Eq. (49)],

$$\hat{E}_{z,l}^{(n)}(r) = \begin{cases} \hat{\phi}_{l,s} J_l(\beta_{l,s} r/R_0) , & 0 \leq r < R_0 , \\ 0 , & \text{otherwise} , \end{cases}$$

where $J_l(x)$ is the Bessel function of the first kind of order l , $\beta_{l,s}$ is the s 'th zero of $J_l(\beta_{l,s}) = 0$ and $\hat{\phi}_{l,s}$ is a constant. In Sec. IV, substituting Eq. (49) into the coupled eigenvalue equations, we obtain closed algebraic dispersion relations for the transverse electric (TE) and transverse magnetic (TM) polarizations.

Introducing the normalized dimensionless function [Eq. (59)],

$$G_{ls}(x) = 4\beta_{l,s}^2 \frac{J_l^2(x)}{(x^2 - \beta_{l,s}^2)^2} ,$$

it is shown in Sec. IV that the coupling between the longitudinal and transverse perturbations is proportional to $G_{ls}(\alpha_{l+1,s} R_0/R_c)$ for the TE mode, and to $G_{ls}(\beta_{l+1,s} R_0/R_c)$ for the TM mode. Here $\alpha_{l+1,s}$ and $\beta_{l+1,s}$ are the s th zeroes of $J'_{l+1}(\alpha_{l+1,s}) = 0$ and $J_{l+1}(\beta_{l+1,s}) = 0$, respectively, R_c is the radius of the outer conducting wall, and the prime denotes $(d/dx)J_l(x)$. Assuming that the maximum of the function $G_{ls}(x)$ occurs at $x = x_{ls}$, we note that the maximum instability growth rate occurs at a value of R_0/R_c given by $R_0/R_c = x_{ls}/\alpha_{l+1,s}$ for the TE mode, and by $R_0/R_c = x_{ls}/\beta_{l+1,s}$ for the TM mode. This result is different from that obtained for a hollow electron beam.⁸

A detailed numerical analysis of the TE mode [Eq. (62)] and TM mode [Eq. (63)] dispersion relations is presented in Sec. IV. Two features are noteworthy from the numerical analysis. First, for the optimized value of R_0/R_c , the instability growth rate for the TM mode is comparable to that for the TE mode. Moreover, the growth rate is reduced substantially by introducing a small amount of axial momentum spread ($\Delta/\gamma_b mc \approx 0.01$).

II. EQUILIBRIUM THEORY AND BASIC ASSUMPTIONS

The equilibrium configuration consists of a relativistic electron beam propagating in the combined transverse wiggler and uniform axial guide fields described by

$$\mathbf{B}^0 = -\delta B \cos(\theta - k_0 z) \hat{\mathbf{e}}_r + \delta B \sin(\theta - k_0 z) \hat{\mathbf{e}}_\theta + B_0 \hat{\mathbf{e}}_z, \quad (1)$$

where B_0 and δB are constants, and k_0 is the axial wavenumber of the helical wiggler field. In Eq. (1), cylindrical polar coordinates (r, θ, z) are used, with z -axis along the propagation direction, and $\hat{\mathbf{e}}_r$, $\hat{\mathbf{e}}_\theta$ and $\hat{\mathbf{e}}_z$ are unit vectors in the r -, θ -, and z -directions, respectively. In the present analysis, we assume that the axial wavenumber of the helical wiggler field is sufficiently large that

$$\left| \frac{\omega_c}{\omega_0 - \omega_c} \right| \left| \frac{\delta B}{B_0} \right| \ll k_0 R_0, \quad (2)$$

where $\omega_0 = k_0 v_b$, $\omega_c = eB_0/\gamma_b mc$ is the electron cyclotron frequency, R_0 is the characteristic beam radius, $\gamma_b mc^2$ is the characteristic electron energy, c is the speed of light in vacuo, $v_b = c(\gamma_b^2 - 1)^{1/2}/\gamma_b$ is the mean axial velocity of the electron beam, and $-e$ and m are the electron charge and rest mass, respectively.

It is also assumed that

$$v/\gamma_b \ll 1, \quad (3)$$

where $v = N_b e^2 / mc^2$ is Budker's parameter,

$$N_b = \int_0^{2\pi} d\theta \int_0^{R_c} dr r n_b^0(r, \theta - k_0 z), \quad (4)$$

is the number of electrons per unit axial length of the beam, $n_b^0(r, \theta - k_0 z)$ is the equilibrium electron density, and R_c is the radius of the conducting wall. The inequality in Eq. (3) indicates that the beam is very tenuous,

and the perturbed electromagnetic fields, to lowest order, are approximated by the vacuum waveguide fields.⁸ Consistent with the low-density assumption in Eq. (3), we also neglect the influence of the (weak) equilibrium self-electric and self-magnetic fields associated with the lack of equilibrium charge and current neutrality.¹²

For present purposes, we assume an equilibrium distribution function of the form¹⁰

$$f_b^0 = \frac{n_0}{\pi} \delta(C_1 - 2\gamma_b m \omega_b C_h - 2\gamma_b m \hat{T}_1) G(C_z), \quad (5)$$

where n_0 , ω_b , and \hat{T}_1 are positive constants, and C_1 , C_h , and C_z are the three single-particle constants of motion defined by¹⁰

$$C_1 = p_r^2 + p_\theta^2 + \frac{2eB_0}{ck_0} (p_z - \gamma_b m v_b) \quad (6)$$

$$- \frac{2e\delta B}{ck_0} p_r \cos(\theta - k_0 z) + \frac{2e\delta B}{ck_0} p_\theta \sin(\theta - k_0 z),$$

$$C_h = p_\theta + \frac{1}{k_0} (p_z - \gamma_b m v_b) + \frac{e\delta B}{ck_0} r \sin(\theta - k_0 z), \quad (7)$$

and

$$\left(C_z - \frac{eB_0}{ck_0} \right)^2 = \left(p_z - \frac{eB_0}{ck_0} \right)^2 \quad (8)$$

$$+ \frac{2e\delta B}{ck_0} p_r \cos(\theta - k_0 z) - \frac{2e\delta B}{ck_0} p_\theta \sin(\theta - k_0 z).$$

The axial distribution function is normalized according to

$$\int_{-\infty}^{\infty} dC_z G(C_z) = 1. \quad (9)$$

In Eqs. (6) - (8), $p_r = (p_r, p_\theta, p_z) = \gamma m \mathbf{v}$ is the mechanical momentum, $p_\theta = r(p_\theta - eB_0 r/2c)$ is the canonical angular momentum associated with the axial field B_0 , and $\gamma m c^2 = (m^2 c^4 + c^2 p_r^2)^{1/2}$ is the relativistic electron energy.

CONVERSATION RECORD		1. DATE 3-4 Sep 81	2. TIME
3. TYPE OF CONVERSATION <input type="checkbox"/> TELEPHONE (Incoming) <input type="checkbox"/> TELEPHONE (Outgoing) <input type="checkbox"/> OFFICE VISIT			
4. SUBJECT OF CONVERSATION <p style="text-align: center;">ARPA Order-3718</p>			
5. CALL/VISIT MADE BY (Name of person)	5a. OFFICE/FIRM/COMPANY, ETC.		5b. PHONE NO. AND OR EXT.
6. CALL/VISIT MADE TO (Name of person)	6a. OFFICE/FIRM/COMPANY, ETC.		6b. PHONE NO. AND OR EXT.
Ms. Spring	ARPA		694 5920
7. SUMMARY OF CONVERSATION, AND IF APPLICABLE, STATEMENT AS TO SUBSEQUENT ACTION TAKEN OR TO BE TAKEN <p style="text-align: center;">Naval Surface Weapons Center, Silver Spring, Md.</p> <p style="text-align: center;">and</p> <p style="text-align: center;">Science Applications, Inc. worked on the above ARPA Order number.</p> <p style="text-align: center;">Document was catalogged to NSWC but the reviewer thought it should go to Science Applications, Inc.</p> <p style="text-align: center;">Either source is correct.</p> <p style="text-align: center;">(IF ADDITIONAL SPACE IS NEEDED, CONTINUE ON REVERSE SIDE)</p>			
8. PRINTED NAME AND TITLE OF PERSON MAKING/RECEIVING CALL/VISIT			8a. SIGNATURE

In the parameter regimes of practical interest for free electron laser applications, the axial distribution function $G(C_z)$ is strongly peaked about $C_z = \gamma_b m V_b = \text{const.}$, with characteristic half-width $\Delta C_z \ll \gamma_b m V_b$. Moreover, in the present analysis, it is also assumed that the axial motion is nonresonant with

$$k_0^2 v_z^2 \neq \omega_c^2, \quad (10)$$

where $v_z = p_z/\gamma m$ is the axial velocity of a typical beam electron. We therefore approximate Eq. (8) by¹⁰

$$C_z = p_z + \frac{\omega_c \delta B}{(\omega_0 - \omega_c) B_0} [p_r \cos(\theta - k_0 z) - p_\theta \sin(\theta - k_0 z)]. \quad (11)$$

Making use of Eqs. (6), (7), and (11), it is straightforward to show that the combination $C_1 - 2\gamma_b m \omega_b C_h$ in Eq. (5) can be expressed as¹⁰

$$\begin{aligned} C_1 - 2\gamma_b m \omega_b C_h = & \left(p_r - \frac{e \delta B}{c k_0} \left(\frac{\omega_0 - \omega_b}{\omega_0 - \omega_c} \right) \cos(\theta - k_0 z) \right)^2 \\ & + \left(p_\theta - \gamma_b m \omega_b r + \frac{e \delta B}{c k_0} \left(\frac{\omega_0 - \omega_b}{\omega_0 - \omega_c} \right) \sin(\theta - k_0 z) \right)^2 \\ & + \gamma_b^2 m^2 \psi_0(r, \theta - k_0 z), \end{aligned} \quad (12)$$

where $\omega_0 = k_0 V_b$, $\omega_c = e B_0 / \gamma_b m c$, and the effective potential $\psi_0(r, \theta - k_0 z)$ is defined by

$$\begin{aligned} \psi_0(r, \theta - k_0 z) = & (\omega_b \omega_c - \omega_b^2) r^2 + 2 \omega_c \omega_b \left(\frac{\omega_c - \omega_b}{\omega_0 - \omega_c} \right) \frac{r}{k_0} \frac{\delta B}{B_0} \sin(\theta - k_0 z) \\ & - \left(\frac{\omega_0 - \omega_b}{\omega_0 - \omega_c} \right)^2 \frac{\omega_c^2}{\omega_0^2} \left(\frac{\delta B}{B_0} \right)^2 v_b^2 + \frac{2}{\gamma_b m} \left(\frac{\omega_c - \omega_b}{\omega_0} \right) v_b (C_z - \gamma_b m V_b). \end{aligned} \quad (13)$$

As a simple example, we consider an axial distribution function in which all electrons have a same value of C_z , i.e.,

$$G(C_z) = \delta(C_z - \gamma_b m v_b) . \quad (14)$$

After some straightforward algebraic manipulation that makes use of Eqs. (5), (12), and (14), it can readily be shown that the lowest-order (azimuthally symmetric) electron density profile described by Eqs. (5) and (14) can be approximated by¹⁰

$$n_b^0(r) = \begin{cases} n_0 , & 0 \leq r \leq R_0 , \\ 0 , & R_0 < r < R_c , \end{cases} \quad (15)$$

where the mean radius R_0 is defined by

$$R_0^2 = \frac{\left(\frac{2\hat{T}_1}{\gamma_b m} + \left(\frac{\omega_0 - \omega_b}{\omega_0 - \omega_c} \right)^2 \frac{\omega_c^2}{\omega_0^2} \left(\frac{\delta B}{B_0} \right)^2 v_b^2 \right)}{(\omega_b \omega_c - \omega_b^2)} , \quad (16)$$

and use has been made of Eq. (2). Additional general equilibrium properties associated with the distribution function in Eq. (5), including helical distortions of the beam equilibrium for finite $\delta B/B_0$, are discussed in Ref. 10.

III. LINEARIZED VLASOV-MAXWELL EQUATIONS FOR A TENUOUS BEAM

In this section, we make use of the linearized Vlasov-Maxwell equations to investigate the free electron laser stability properties of a relativistic solid electron beam described by the equilibrium distribution function in Eq. (5). We adopt a normal-mode approach in which all perturbations are assumed to vary with time and space according to

$$\delta\psi(\mathbf{x}, t) = \sum_{\ell, n} \hat{\psi}_{\ell}^{(n)}(\mathbf{r}) \exp\{i[\ell\theta + (k + nk_0)z - \omega t]\}, \quad (17)$$

where $\text{Im}\omega > 0$. Here, ω is the complex eigenfrequency, $k + nk_0$ is the axial wavenumber, and ℓ and n are integers. Moreover, it is also assumed that the perturbations are close to resonance with

$$|\omega - (k + nk_0)v_b| \ll \omega_0, \omega_c, \quad (18)$$

where $\omega_0 = k_0 v_b$ and $\omega_c = eB_0/\gamma_b mc$.

The Maxwell equations for the perturbed electric and magnetic field amplitudes can be expressed as

$$\nabla \times \hat{\mathbf{E}}(\mathbf{x}) = i(\omega/c)\hat{\mathbf{B}}(\mathbf{x}), \quad (19)$$

$$\nabla \times \hat{\mathbf{B}}(\mathbf{x}) = (4\pi/c)\hat{\mathbf{J}}(\mathbf{x}) - i(\omega/c)\hat{\mathbf{E}}(\mathbf{x}),$$

where

$$\hat{\mathbf{J}}(\mathbf{x}) = -e \int d^3p \nabla \hat{f}_b(\mathbf{x}, \mathbf{p}), \quad (20)$$

is the perturbed current density. In Eq. (20),

$$\hat{f}_b(\mathbf{x}, \mathbf{p}) = e \int_{-\infty}^0 d\tau \exp(-i\omega\tau) \left(\hat{\mathbf{E}}(\mathbf{x}') + \frac{\mathbf{x}' \times \hat{\mathbf{B}}(\mathbf{x}')}{c} \right) \cdot \frac{\partial}{\partial \mathbf{p}'} f_b^0, \quad (21)$$

is the perturbed distribution function, $\tau = t' - t$, and the particle trajectories $\chi'(t')$ and $p'(t')$ satisfy $d\chi'/dt' = \chi'$ and $dp'/dt' = -e\chi' \times \hat{k}^0/c$, with "initial" conditions $\chi'(t' = t) = \chi$ and $p'(t' = t) = p$.

Within the context of Eqs. (3) and (18), the perturbed distribution function in Eq. (21) can be approximated by

$$\begin{aligned} \hat{f}_b(\chi, p) = & -\frac{ie}{\omega} \int_{-\infty}^0 d\tau \exp(-i\omega\tau) \left\{ 2 \left(\gamma m i \omega (\chi' \cdot \hat{k}) \right. \right. \\ & \left. \left. - p_z \left(\chi' \cdot \frac{\partial}{\partial z} \hat{k} \right) \right) \frac{\partial}{\partial p_z^2} f_b^0 + \left(\chi' \cdot \frac{\partial}{\partial z} \hat{k} \right) \frac{\partial}{\partial p_z} f_b^0 \right\}, \end{aligned} \quad (22)$$

where $\gamma = (1 + p^2/m^2 c^2)^{1/2}$, and use has been made of Eq. (19). To lowest order, the axial motion of an electron is free-streaming with¹⁰

$$z' = z + \frac{p_z}{\gamma m} (t' - t). \quad (23)$$

Moreover, within the context of Eq. (18), on the right-hand side of Eq. (22) we retain contributions to v_r' and v_θ' in the orbit integral of the form⁸

$$v_r' = v_z \frac{\omega_c}{\omega_0 - \omega_c} \frac{\delta B}{B_0} \cos(\theta - k_0 z - k_0 v_z \tau), \quad (24)$$

and

$$v_\theta' = -v_z \frac{\omega_c}{\omega_0 - \omega_c} \frac{\delta B}{B_0} \sin(\theta - k_0 z - k_0 v_z \tau). \quad (25)$$

Finally, since the oscillatory modulation of the radial and azimuthal orbits is small amplitude [Eq. (2)], we approximate

$$r' = r, \quad \theta' = \theta, \quad (26)$$

in the arguments of the perturbation amplitudes on the right-hand side of Eq. (22).

Substituting Eqs. (23) - (26) into Eq. (22), we obtain the perturbed distribution function

$$\begin{aligned} \hat{f}_b(x, p) &= \sum_{\ell, n} \hat{f}_{b\ell}^{(n)} \exp\{i[\ell\theta + (k + nk_0)z]\} \\ &= \frac{iec}{\omega} \sum_{\ell, n} \frac{\exp\{i[\ell\theta + (k + nk_0)z]\}}{\omega - (k + nk_0)v_z} \left(\lambda_n \beta_z \hat{E}_{z, \ell}^{(n)}(r) + \frac{e\delta B}{2\gamma mc^2 k_0} \frac{\omega_0}{\omega_0 - \omega_c} \right. \\ &\quad \times \left. \left\{ \lambda_{n+1} [\hat{E}_{r, \ell-1}^{(n+1)}(r) + i\hat{E}_{\theta, \ell-1}^{(n+1)}(r)] + \lambda_{n-1} [\hat{E}_{r, \ell+1}^{(n-1)}(r) - i\hat{E}_{\theta, \ell+1}^{(n-1)}(r)] \right\} \right), \end{aligned} \quad (27)$$

where the function $\lambda_n(p, \omega, k)$ is defined by

$$\lambda_n(p, \omega, k) = 2[\gamma m \omega - (k + n'k_0)p_z] \frac{\partial f_b^0}{\partial p_z} + (k + n'k_0) \frac{\partial f_b^0}{\partial p_z}, \quad (28)$$

and $\beta_z = v_z/c$. In Eq. (27), the term proportional to λ_n is the longitudinal portion of the perturbed distribution function.

Similarly, the terms proportional to λ_{n+1} and λ_{n-1} in Eq. (27) are the transverse electromagnetic portions of the perturbed distribution function.

Consistent with Eq. (18), the eigenfrequency ω can be approximated by $\omega = (k + nk_0)v_b$. We therefore approximate $\omega^2/c^2 - (k + nk_0 + k_0)^2$ by

$$\omega^2/c^2 - (k + nk_0 + k_0)^2 \approx - \left(\frac{(k + nk_0)^2}{\gamma_b^2} + 2k_0(k + nk_0) + k_0^2 \right) < 0, \quad (29)$$

for $k + nk_0 > 0$. Evidently, Eq. (29) indicates that the $n + 1$ mode in Eq. (27) is a non-propagating wave in a vacuum waveguide. Without loss of generality, for a tenuous beam, we therefore assume

$$\hat{E}_{r, \ell-1}^{(n+1)}(r) = \hat{E}_{\theta, \ell-1}^{(n+1)}(r) = 0, \quad (30)$$

in the subsequent analysis. Making use of Eq. (30), $\hat{f}_b(x, p)$ in Eq. (27) can then be expressed as

$$\hat{f}_b(x, \rho) = \frac{ie\epsilon}{\omega} \sum_{l,n} \frac{\exp\{i[l\theta + (k + nk_0)z]\}}{\omega - (k + nk_0)v_z} \left\{ \lambda_{n\beta} \hat{E}_{z,l}^{(n)}(r) + \Lambda \lambda_{n-1} [\hat{E}_{r,l+1}^{(n-1)}(r) - i\hat{E}_{\theta,l+1}^{(n-1)}(r)] \right\}, \quad (31)$$

where the dimensionless parameter Λ is defined by

$$\Lambda = \frac{e\delta B}{2\gamma_b mc^2 k_0} \frac{\omega_0}{\omega_0 - \omega_c}, \quad (32)$$

and use has been made of the approximation $\gamma = \gamma_b$, which is consistent with Eq. (18).

From Poisson's equation, $\nabla \cdot \hat{E}(x) = 4\pi\hat{\rho}(x)$, and the Maxwell equation (19), we obtain the differential equation,

$$\left[\nabla_{\perp}^2 + \frac{\omega^2}{c^2} - (k + nk_0)^2 \right] \hat{E}_{z,l}^{(n)}(r) = \frac{4\pi i(k + nk_0)}{\gamma_b^2} \hat{\rho}_l^{(n)}(r), \quad (33)$$

for the axial (longitudinal) component of the perturbed electric field $\hat{E}_{z,l}^{(n)}$. In Eq. (33), $\hat{\rho}_l^{(n)}(r) = -e \int d^3p f_{bl}^{(n)}$ is the perturbed charge density, $\nabla_{\perp}^2 \equiv r^{-1}(\partial/\partial r)(r\partial/\partial r) - l^2/r^2$, and use has been made of $\hat{j}_{z,l}^{(n)}(r) = v_b \hat{\rho}_l^{(n)}(r)$. In the tenuous beam limit [Eq. (3)], the transverse field components $\hat{E}_{r,l+1}^{(n-1)}(r)$ in Eq. (31) can be approximated by the vacuum waveguide fields.⁸ In this context, the present stability analysis utilizes the vacuum transverse electric (TE) and transverse magnetic (TM) waveguide modes as a convenient basis to represent the general electromagnetic field perturbation $\hat{E}_{r,l+1}^{(n-1)}(r)$, which is determined from¹¹

$$\left[\frac{\omega^2}{c^2} - (k + nk_0 - k_0)^2 \right] \hat{E}_{r,l+1}^{(n-1)}(x) = \nabla_{\perp} \frac{\partial}{\partial z} \hat{E}_{z,l+1}^{(n-1)}(x) - i \frac{\omega}{c} \hat{e}_z \times \nabla_{\perp} \hat{B}_{z,l+1}^{(n-1)}(x). \quad (34)$$

Making use of Eqs. (19) and (34), and neglecting the perturbed current density, the vacuum waveguide fields can be expressed as

$$\begin{aligned}\hat{B}_{z,\ell+1}^{(n-1)}(r) &= b_{\ell+1,s} J_{\ell+1}(\alpha_{\ell+1,s} r/R_c), \\ \hat{E}_{r,\ell+1}^{(n-1)}(r) - i\hat{E}_{\theta,\ell+1}^{(n-1)}(r) &= -\frac{\omega R_c}{c\alpha_{\ell+1,s}} b_{\ell+1,s} J_{\ell}(\alpha_{\ell+1,s} r/R_c),\end{aligned}\quad (35)$$

for the TE mode, and

$$\begin{aligned}\hat{E}_{z,\ell+1}^{(n-1)}(r) &= \epsilon_{\ell+1,s} J_{\ell+1}(\beta_{\ell+1,s} r/R_c), \\ \hat{E}_{r,\ell+1}^{(n-1)}(r) - i\hat{E}_{\theta,\ell+1}^{(n-1)}(r) &= i \frac{(k + nk_0 - k_0)R_c}{\beta_{\ell+1,s}} \epsilon_{\ell+1,s} J_{\ell}(\beta_{\ell+1,s} r/R_c),\end{aligned}\quad (36)$$

for the TM mode. In Eqs. (35) and (36), $b_{\ell+1,s}$ and $\epsilon_{\ell+1,s}$ are constants, $J_{\ell}(x)$ is the Bessel function of first kind of order ℓ , and $\alpha_{\ell+1,s}$ and $\beta_{\ell+1,s}$ are the s th roots of $J'_{\ell+1}(\alpha_{\ell+1,s}) = 0$ and $J_{\ell+1}(\beta_{\ell+1,s}) = 0$, respectively. Here the prime (') denotes $J'_{\ell+1}(x) = (d/dx)J_{\ell+1}(x)$. After some straightforward algebraic manipulation of Eqs. (19), (35), and (36), it can be shown that

$$\begin{aligned}&\left\{ \frac{\omega^2}{c^2} - (k + nk_0 - k_0)^2 - \frac{\alpha_{\ell+1,s}^2}{R_c^2} \right\} b_{\ell+1,s} J_{\ell+1}\left(\frac{\alpha_{\ell+1,s} r}{R_c}\right) \\ &= -\frac{4\pi}{rc} \left\{ \frac{\partial}{\partial r} [r \hat{J}_{\theta,\ell+1}^{(n-1)}(r)] - i(\ell+1) \hat{J}_{r,\ell+1}^{(n-1)}(r) \right\},\end{aligned}\quad (37)$$

for the TE mode, and

$$\begin{aligned}&\left\{ \frac{\omega^2}{c^2} - (k + nk_0 - k_0)^2 - \frac{\beta_{\ell+1,s}^2}{R_c^2} \right\} \epsilon_{\ell+1,s} J_{\ell+1}\left(\frac{\beta_{\ell+1,s} r}{R_c}\right) \\ &= 4\pi i \left\{ (k + nk_0 - k_0) \hat{\rho}_{\ell+1}^{(n-1)}(r) - \frac{\omega}{c^2} \hat{J}_{z,\ell+1}^{(n-1)}(r) \right\},\end{aligned}\quad (38)$$

for the TM mode. Moreover, making use of the continuity equation,

$$i\omega \hat{\rho}_{\ell+1}^{(n-1)} - i(k + nk_0 - k_0) \hat{J}_{z,\ell+1}^{(n-1)} = \frac{1}{r} \frac{\partial}{\partial r} [r \hat{J}_{r,\ell+1}^{(n-1)}] + \frac{i(\ell+1)}{r} \hat{J}_{\theta,\ell+1}^{(n-1)},\quad (39)$$

the approximation $\hat{J}_{z,\ell+1}^{(n-1)}(r) = v_b \hat{J}_{\ell+1}^{(n-1)}(r)$ [consistent with Eq. (3)], and approximating $k + nk_0 = k_0/(1 - v_b/c)$ on the right-hand side of Eq. (38), we find that Eq. (38) can be expressed as

$$\left(\frac{\omega^2}{c^2} - (k + nk_0 - k_0)^2 - \frac{\beta_{\ell+1,s}^2}{R_c^2} \right) \epsilon_{\ell+1,s} J_{\ell+1} \left(\frac{\beta_{\ell+1,s} r}{R_c} \right) = \frac{4\pi}{rc} \left\{ \frac{\partial}{\partial r} [r \hat{J}_{r,\ell+1}^{(n-1)}(r)] + i(\ell+1) \hat{J}_{\theta,\ell+1}^{(n-1)}(r) \right\}, \quad (40)$$

for the TM mode.

For convenience of notation in the subsequent analysis, we introduce the effective susceptibility,

$$\chi_{n,n}(\omega, k) = 4\pi e^2 \int d^3p \frac{\lambda_{n'}(p, \omega, k)}{\omega - (k + nk_0)v_z}. \quad (41)$$

Moreover, to simplify the present analysis, we also assume that the beam rotation is slow with

$$\omega_b \ll \omega_c, \omega_0. \quad (42)$$

Within the context of Eq. (42), we can show from Eq. (12) that the equilibrium distribution function is an even function of

$$p_r - 2\gamma_b mc \Lambda \cos(\theta - k_0 z) \quad (43)$$

and

$$p_\theta + 2\gamma_b mc \Lambda \sin(\theta - k_0 z), \quad (44)$$

for the beam rotations satisfying $\omega_b \ll \omega_c, \omega_0$. Making use of Eqs. (31), (41), and (43), the perturbed charge and current densities are given by

$$\hat{J}_{\theta,\ell+1}^{(n-1)}(r) = \frac{c^2 \Lambda}{4\pi\omega} G_\ell(\omega, k, r) = i \hat{J}_{r,\ell+1}^{(n-1)}(r) = ic \Lambda \hat{\rho}_\ell^{(n)}(r), \quad (45)$$

where the function $G_\ell(\omega, k, r)$ is defined by

$$G_l(\omega, k, r) = \chi_{n,n} \beta_z \hat{E}_{z,l}^{(n)}(r) + \Lambda \chi_{n,n-1} [\hat{E}_{r,l+1}^{(n-1)}(r) - i \hat{E}_{\theta,l+1}^{(n-1)}(r)] . \quad (46)$$

Equations (33), (37), and (40), when combined with Eq. (45), constitute one of the principal results of this paper and can be used to investigate stability properties for a broad range of system parameters. Moreover, in limiting cases, the dispersion relation for the free electron laser instability can be obtained in a closed form (Sec. IV).

IV. FREE ELECTRON LASER STABILITY PROPERTIES

In this section, simplified expressions are obtained for the longitudinal perturbations in Eq. (33), and the results are used to derive the dispersion relation for several values of azimuthal harmonic number l .

The present analysis assumes short wavelength perturbations with

$$|q_n^2| = |(k + nk_0)^2 - \omega^2/c^2| \gg 1/R_0^2. \quad (47)$$

Moreover, for $\omega \approx (k + nk_0)V_b$ and $k + nk_0 \approx k_0/(1 - V_b/c)$, the inequality in Eq. (47) can be expressed in the equivalent form,

$$(1 + V_b/c)^2 \gamma_b^2 k_0^2 R_0^2 \gg 1, \quad (48)$$

which is readily satisfied in the parameter regimes of present experimental interest. As shown in Appendix A, for short wavelength perturbations satisfying Eq. (48), the axial component of the perturbed electric field $\hat{E}_{z,l}^{(n)}(r)$ in Eq. (33) can be approximated by

$$\hat{E}_{z,l}^{(n)}(r) = \begin{cases} \hat{\phi}_{l,s} J_l(\beta_{l,s} r/R_0), & 0 \leq r < R_0, \\ 0, & \text{otherwise.} \end{cases} \quad (49)$$

In Eq. (49), $\beta_{l,s}$ is the s 'th root of $J_l(\beta_{l,s}) = 0$, and $\hat{\phi}_{l,s}$ is a constant.

Substituting Eqs. (35) and (49) into Eq. (46), multiplying Eqs. (33) and (37) by $r J_l(\beta_{l,s} r/R_0)$ and $r J_{l+1}(\alpha_{l+1,s} r/R_c)$, respectively, and integrating from $r = 0$ to $r = R_c$, we obtain two homogeneous equations relating the perturbation amplitudes $\hat{\phi}_{l,s}$ and $b_{l+1,s}$. For the TE mode polarization, these are

$$\hat{\phi}_{l,s} \int_0^{R_c} dr r \Theta(R_0 - r) \left(\frac{1}{2} \chi_{n,n} + q_n^2 + \frac{\beta_{l,s}^2}{R_0^2} \right) J_l^2 \left(\frac{\beta_{l,s} r}{R_0} \right) \quad (50)$$

$$\begin{aligned}
&= \frac{(k + nk_0)R_c}{\gamma_b^2 \epsilon_{l+1,s}} \int_0^{R_c} dr r \chi_{n,n-1} J_l \left(\frac{\alpha_{l+1,s} r}{R_c} \right) J_l \left(\frac{\beta_{l,s} r}{R_0} \right), \\
\text{and} \\
&\epsilon_{l+1,s} \int_0^{R_c} dr r \left[\frac{\omega^2}{c^2} - (k + nk_0 - k_0)^2 - \frac{\alpha_{l+1,s}^2}{R_c^2} + \lambda^2 \chi_{n,n-1} \right] J_{l+1}^2 \left(\frac{\alpha_{l+1,s} r}{R_c} \right) \\
&= \frac{\beta_{l,s}}{(k + nk_0)R_0} \lambda \hat{\phi}_{l,s} \int_0^{R_c} dr r \Theta(R_0 - r) \chi_{n,n} J_l \left(\frac{\beta_{l,s} r}{R_0} \right) J_{l+1} \left(\frac{\alpha_{l+1,s} r}{R_c} \right), \quad (51)
\end{aligned}$$

where $\Theta(x)$ is the Heaviside step function defined by

$$\Theta(x) = \begin{cases} 1, & x > 0, \\ 0, & \text{otherwise.} \end{cases} \quad (52)$$

Similarly, for the TM mode polarization, we obtain

$$\begin{aligned}
&\hat{\phi}_{l,s} \int_0^{R_c} dr r \Theta(R_0 - r) \left(\frac{1}{\gamma_b^2} \chi_{n,n} + q_n^2 + \frac{\beta_{l,s}^2}{R_0^2} \right) J_l^2 \left(\frac{\beta_{l,s} r}{R_0} \right) \\
&= -i \frac{(k + nk_0)R_c}{\gamma_b^2 \epsilon_{l+1,s}} \lambda \epsilon_{l+1,s} \int_0^{R_c} dr r \chi_{n,n-1} J_l \left(\frac{\alpha_{l+1,s} r}{R_c} \right) J_l \left(\frac{\beta_{l,s} r}{R_0} \right), \quad (53)
\end{aligned}$$

and

$$\begin{aligned}
&\epsilon_{l+1,s} \int_0^{R_c} dr r \left[\frac{\omega^2}{c^2} - (k + nk_0 - k_0)^2 - \frac{\beta_{l+1,s}^2}{R_c^2} + \lambda^2 \chi_{n,n-1} \right] J_{l+1}^2 \left(\frac{\beta_{l+1,s} r}{R_c} \right) \\
&= i \frac{\beta_{l,s}}{(k + nk_0)R_0} \lambda \hat{\phi}_{l,s} \int_0^{R_c} dr r \Theta(R_0 - r) \chi_{n,n} J_{l+1} \left(\frac{\beta_{l,s} r}{R_0} \right) \\
&\quad \times J_{l+1} \left(\frac{\alpha_{l+1,s} r}{R_c} \right), \quad (54)
\end{aligned}$$

where use has been made of $\omega = (k + nk_0)v_b$ and $(k + nk_0) = k_0/(1 - v_b/c)$.

In the present analysis, it is assumed that the axial distribution function has the form

$$G(C_z) = \frac{\Delta}{\pi} \frac{1}{(C_z - \gamma_b m v_b)^2 + \Delta^2}, \quad (55)$$

where Δ is the characteristic spread in C_z about the mean value $C_z = \gamma_b m v_b$.

We further assume that the characteristic spread Δ is small in comparison with $\gamma_b m v_b$. Substituting Eqs. (5) and (55) into Eqs. (28) and (41), we obtain the approximate expression

$$\chi_{n,n'} = \begin{cases} \frac{4\nu}{\gamma_b R_0^2} \frac{\omega^2 - (k + nk_0)(k + n'k_0)c^2}{[\omega - (k + nk_0)v_b + i|k + nk_0|\Delta/\gamma_b^3]^2}, & 0 \leq r < R_0, \\ 0, & R_0 < r \leq R_c \end{cases} \quad (56)$$

In obtaining Eq. (56), use has been made of Eq. (18). Making use of the definition of Budker's parameter in Eqs. (3) and (4), the term $4\nu/\gamma_b R_0^2$ in Eq. (56) can also be expressed as $4\nu/\gamma_b R_0^2 = \omega_{pb}^2/c^2$, where $\omega_{pb}^2 = 4\pi n_0 e^2/\gamma_b m$ is the plasma frequency-squared.

The condition for a nontrivial solution to Eqs. (50) and (51) is that the determinant of the coefficients $\hat{c}_{l,s}$, and $b_{l+1,s}$ be equal to zero. After some algebraic manipulation, we find that the TE mode dispersion relation can be expressed as

$$\begin{aligned} & \left[\omega - (k + nk_0)v_b + i \frac{|k + nk_0|\Delta}{\gamma_b^3} \right]^2 \left\{ \frac{\omega^2}{c^2} - (k + nk_0 - k_0)^2 - \frac{\alpha_{l+1,s}^2}{R_c^2} \right\} \\ & \times \left\{ \left[\omega - (k + nk_0)v_b + i \frac{|k + nk_0|\Delta}{\gamma_b^3} \right]^2 - 4 \frac{\nu c^2}{\gamma_b R_0^2} \right\} \\ & = 4\lambda^2 \frac{\nu c^2}{\gamma_b R_c^2} \left[k_0(k + nk_0 - k_0) - \frac{\alpha_{l+1,s}^2}{R_c^2} \right] Q_{lss}^E \left(\frac{\alpha_{l+1,s} R_0}{R_c} \right) \left\{ 4 \frac{\nu c^2}{\gamma_b R_0^2} \right. \\ & + H_{lss} \left(\frac{\alpha_{l+1,s} R_0}{R_c} \right) \left[\omega - (k + nk_0)v_b + i \frac{|k + nk_0|\Delta}{\gamma_b^3} \right]^2 \\ & \left. - 4 \frac{\nu c^2}{\gamma_b R_0^2} H_{lss} \left(\frac{\alpha_{l+1,s} R_0}{R_c} \right) \right\}, \end{aligned} \quad (57)$$

where the coupling coefficient $Q_{lss}^E(\alpha_{l+1,s} R_0/R_c)$ is defined by

$$Q_{lss}^E(x) = \frac{\alpha_{l+1,s}^2}{\alpha_{l+1,s}^2 - (l+1)^2} \frac{G_{ls}(x)}{J_{l+1}^2(\alpha_{l+1,s})}, \quad (58)$$

and the functions $G_{ls}(x)$ and $H_{lss}(x)$ are defined by

$$G_{ls},(x) = 4\beta_{ls}^2 \frac{J_l^2(x)}{(x^2 - \beta_{ls}^2)^2} \quad (59)$$

and

$$h_{lss},(x) = \frac{J_{l+1}^2(x) - J_l(x)J_{l+2}(x)}{G_{ls},(x)} \quad (60)$$

In Eq. (57), the subscript s and s' represent the radial mode numbers of the transverse and longitudinal perturbations, respectively.

For small wiggler amplitude ($\Delta \ll 1$), we investigate free electron laser stability properties for ω and $k + nk_0$ near the simultaneous zeros of the transverse dispersion relation, $\omega^2 - (k + nk_0 - k_0)^2 c^2 - \alpha_{l+1,s}^2 c^2 / R_c^2 = 0$, and the longitudinal dispersion relation

$$\left[\omega - (k + nk_0)V_b + i \frac{|k + nk_0|\Delta}{\gamma_b^3} \right]^2 - 4 \frac{vc^2}{\gamma_b^3 R_0^2} = 0 \quad (61)$$

In this regard, making use of Eq. (61), the TE mode dispersion relation in Eq. (57) can be approximated by

$$\left\{ \frac{\omega^2}{c^2} - (k + nk_0 - k_0)^2 - \frac{\alpha_{l+1,s}^2}{R_c^2} \right\} \left\{ \left[\omega - (k + nk_0)V_b + i \frac{|k + nk_0|\Delta}{\gamma_b^3} \right]^2 - 4 \frac{vc^2}{\gamma_b^3 R_0^2} \right\} = 4\Delta^2 \frac{vc^2}{\gamma_b^3 R_c^2} \left[k_0(k + nk_0 - k_0) - \frac{\alpha_{l+1,s}^2}{R_c^2} \right] Q_{lss}^E \left(\frac{\alpha_{l+1,s} R_0}{R_c} \right) \quad (62)$$

In a similar manner, from Eqs. (53) and (54), we obtain the approximate TM mode dispersion relation,

$$\left\{ \frac{\omega^2}{c^2} - (k + nk_0 - k_0)^2 - \frac{\beta_{l+1,s}^2}{R_c^2} \right\} \left\{ \left[\omega - (k + nk_0)V_b + i \frac{|k + nk_0|\Delta}{\gamma_b^3} \right]^2 - 4 \frac{vc^2}{\gamma_b^3 R_0^2} \right\} = 4\Delta^2 \frac{vc^2}{\gamma_b^3 R_c^2} \left[k_0(k + nk_0 - k_0) - \frac{\beta_{l+1,s}^2}{R_c^2} \right] Q_{lss}^M \left(\frac{\beta_{l+1,s} R_0}{R_c} \right) \quad (63)$$

where the TM mode coupling coefficient $Q_{lss}^M(\beta_{l+1,s} R_0 / R_c)$ is defined by

$$Q_{lss}^M(x) = G_{ls},(x) / J_{l+2}^2(\beta_{l+1,s}) \quad (64)$$

and the function $G_{ls},(x)$ is defined in Eq. (59).

Figure 1 shows plots of $G_{ls}(x)$ versus x obtained from Eq. (59) for (a) $\beta_{l,s'} = \beta_{0,1}$ and (b) $\beta_{l,s'} = \beta_{1,3}$. Except in the case $\beta_{l,s'} = \beta_{0,1}$, the plots of $G_{ls}(x)$ for arbitrary $\beta_{l,s'}$ are similar to those for $\beta_{l,s'} = \beta_{1,3}$ in Fig. 1(b). As shown in Fig. 1(b), the quantities $G_{ls}^\phi \equiv G_{ls}(x_{ls})$ and x_{ls} denote the maximum value of $G_{ls}(x)$ and the corresponding value of x for a specified $\beta_{l,s'}$. For example, in Fig. 1, $(x_{ls}, G_{ls}^\phi) = (0, 0.69)$ for $\beta_{l,s'} = \beta_{0,1}$ and $(x_{ls}, G_{ls}^\phi) = (9.8, 0.064)$ for $\beta_{l,s'} = \beta_{1,3}$. Shown in Fig. 2 are plots of (a) x_{ls} and (b) the corresponding values of $G_{ls}^\phi = G_{ls}(x_{ls})$ for several different values of the azimuthal and radial mode numbers l and s' . It is evident from Fig. 2(b) that G_{ls}^ϕ decreases rapidly with increasing values of the mode numbers l and s' . Moreover, we note from Fig. 2(a) that x_{ls} can be approximated by

$$x_{ls'} \approx \beta_{l,s'}, \quad s' \neq 1. \quad (65)$$

In this regard, for $s' \neq 1$, G_{ls}^ϕ can be approximated by

$$G_{ls'}^\phi \approx G_{ls}(\beta_{l,s'}) = J_{l+1}^2(\beta_{l,s'}), \quad s' \neq 1. \quad (66)$$

Shown in Fig. 3 are plots of (a) $Q_{lss'}^E/G_{ls}$, for the TE mode and (b) $Q_{lss'}^M/G_{ls}$, for the TM mode, obtained from Eqs. (58) and (64) respectively. Note that the curves in Fig. 3 are independent of the longitudinal radial mode number s' . Evidently, the values of $Q_{lss'}^E/G_{ls}$ and $Q_{lss'}^M/G_{ls}$ increase with increasing values of azimuthal and transverse radial mode numbers, l and s . After careful examination of Eqs. (58) and (64), we find that the maximum coupling between the transverse and longitudinal modes occurs for a value of R_0/R_c given by

$$R_0/R_c = \begin{cases} x_{ls}'/\alpha_{l+1,s} & \text{TE mode} \\ x_{ls}'/\beta_{l+1,s} & \text{TM mode} \end{cases} \quad (67)$$

Equation (67) is valid only when $x_{ls}' \leq \alpha_{l+1,s}$ for the TE mode, and $x_{ls}' \leq \beta_{l+1,s}$ for the TM mode. For $x_{ls}' > \alpha_{l+1,s}$ (TE), or $x_{ls}' > \beta_{l+1,s}$ (TM), the maximum coupling occurs for $R_0/R_c = 1$. The maximum coupling coefficients corresponding to Eq. (67) can be determined from Figs. 2(b) and 3. For example, for $(l,s,s') = (3,2,1)$, we determine that the maximum coupling coefficient and the corresponding ratio R_0/R_c are given by $(Q_{lss}'^E, R_0/R_c) = (1.607, 0.625)$ for the TE mode, and $(Q_{lss}'^M, R_0/R_c) = (1.83, 0.52)$ for the TM mode.

It is instructive to examine the present results for perturbations with the lowest mode numbers, i.e., $(l,s,s') = (0,1,1)$, particularly for a beam-filled waveguide with $R_0/R_c = 1$. In this limit, from Fig. 1(a), we obtain $G_{ls}'(\alpha_{1,1}) = 0.4$ for the TE mode, and $G_{ls}'(\beta_{1,1}) = 0.045$ mode. We therefore conclude that the TE mode polarization is the most unstable. Multiplying $G_{ls}'(\alpha_{1,1}) = 0.4$ by $Q_{lss}'^E/G_{ls}' = 4.2$ in Fig. 3(a), the coupling coefficient is given by $Q_{011}^E = 1.7$. Assuming zero axial momentum spread ($\Delta = 0$) and short axial wavelengths ($k_0^2 R_c^2 \gg 1$), the TE mode dispersion relation in Eq. (62) can be approximated by

$$\left(\frac{\omega^2}{c^2} - (k + nk_0 - k_0)^2 \right) \left\{ [\omega - (k + nk_0)V_b]^2 - \frac{\omega_{pb}^2}{\gamma_b^2} \right\} = 3.4 \lambda^2 \omega_{pb}^2 k_0^2, \quad (68)$$

for the $(l,s,s') = (0,1,1)$ perturbation and $R_0/R_c = 1$. Equation (68) is similar in form to the result obtained by Davidson and Uhm³ for a uniform density beam with infinite cross section. In particular, the constant numerical factor on the right-hand side of Eq. (68) is equal to 3.4, whereas in Ref. 3 the constant numerical factor is equal to 8.

Finally, we have investigated detailed stability properties by solving the dispersion relations in Eqs. (62) and (63) numerically for a broad range of system parameters. Defining the normalized Doppler-shifted eigenfrequency by

$$\Omega = [\omega - (k + nk_0)v_b]/k_0c, \quad (69)$$

we calculate the normalized growth rate $\Omega_i = \text{Im}\Omega$ from Eqs. (62) and (63). Shown in Fig. 4 are plots of the normalized growth rate Ω_i versus $(k + nk_0)/k_0$ for $(\ell, s, s') = (3, 2, 1)$, $k_0R_c = 10$, $\gamma_b = 10$, $v/\gamma_b = 0.02$, and $\Lambda^2 = 0.01$, with (a) $R_0/R_c = x_{31}/\alpha_{4,2}$ for the TE mode, and (b) $R_0/R_c = x_{31}/\beta_{4,2}$ for the TM mode. For these optimized choices of R_0/R_c , the instability growth rate for the TM mode is comparable to that for the TE mode. Moreover, the growth rate is reduced substantially by introducing a small amount of axial momentum spread ($\Delta/\gamma_b mc \approx 0.01$).

We conclude this section by pointing out two areas in which the analysis can be extended. First, the restriction to very short wavelength perturbations [Eq. (46)] can be removed in a relatively straightforward manner. Second, paralleling the self-consistent theoretical formalism developed in previous studies,⁸ the stability analysis can also be carried out without making the approximation that the transverse perturbations are represented by the vacuum waveguide fields.

V. CONCLUSIONS

In this paper, we have examined the free electron laser instability for a solid relativistic electron beam propagating in the combined transverse wiggler and uniform axial guide field given in Eq. (1). The analysis was carried out within the framework of the linearized Vlasov-Maxwell equations. The equilibrium (Sec. II) and stability (Secs. III and IV) properties were investigated in detail for the choice of distribution function in which all electrons have the same value of the linear combination of transverse and helical invariants, $C_1 - 2\gamma_b m\omega_b C_h$, and a Lorentzian distribution in the axial invariant C_z [Eqs. (5) and (18)]. One of the most important conclusions of this analysis is that the maximum instability growth rate for a solid electron beam is comparable to that of a hollow beam with similar parameters.⁸ Moreover, it is also found that the maximum growth rate occurs at a value of R_0/R_c corresponding to $R_0/R_c = x_{ls}/a_{l+1,s}$ for TE mode perturbations, and $R_0/R_c = x_{ls}/b_{l+1,s}$ for TM mode perturbations. For these optimized values of R_0/R_c , the instability growth rate for the TM mode is comparable to that for the TE mode. Moreover, the growth rate is substantially reduced by introducing a small amount of axial momentum spread ($\Delta/\gamma_b mc \sim 0.01$).

ACKNOWLEDGMENTS

This research was supported in part by Defense Advance Research Project Agency (DOD) under ARPA Order No. 3718, Amendment No. 12, in part by the Independent Research Fund at the Naval Surface Weapons Center, and in part by the Office of Naval Research.

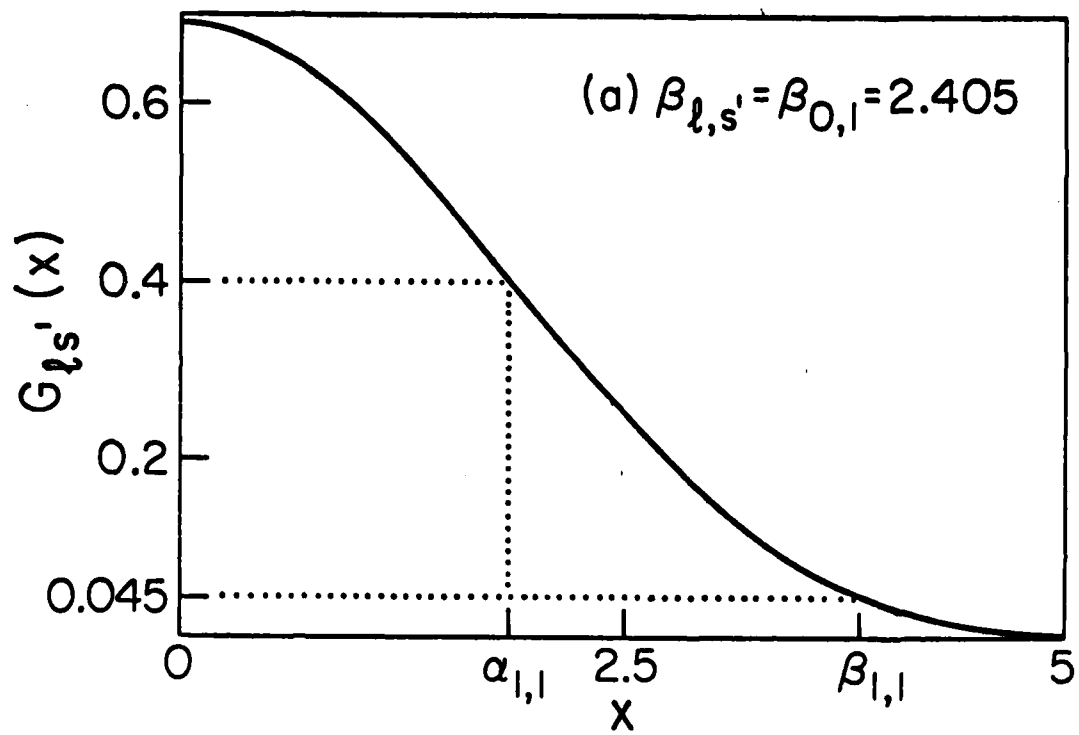


FIGURE 1(a) PLOTS OF $G_{\ell s'}(x)$ VERSUS x EQ.(59) FOR (a) $\beta_{\ell, s'} \equiv \beta_{0,1}$

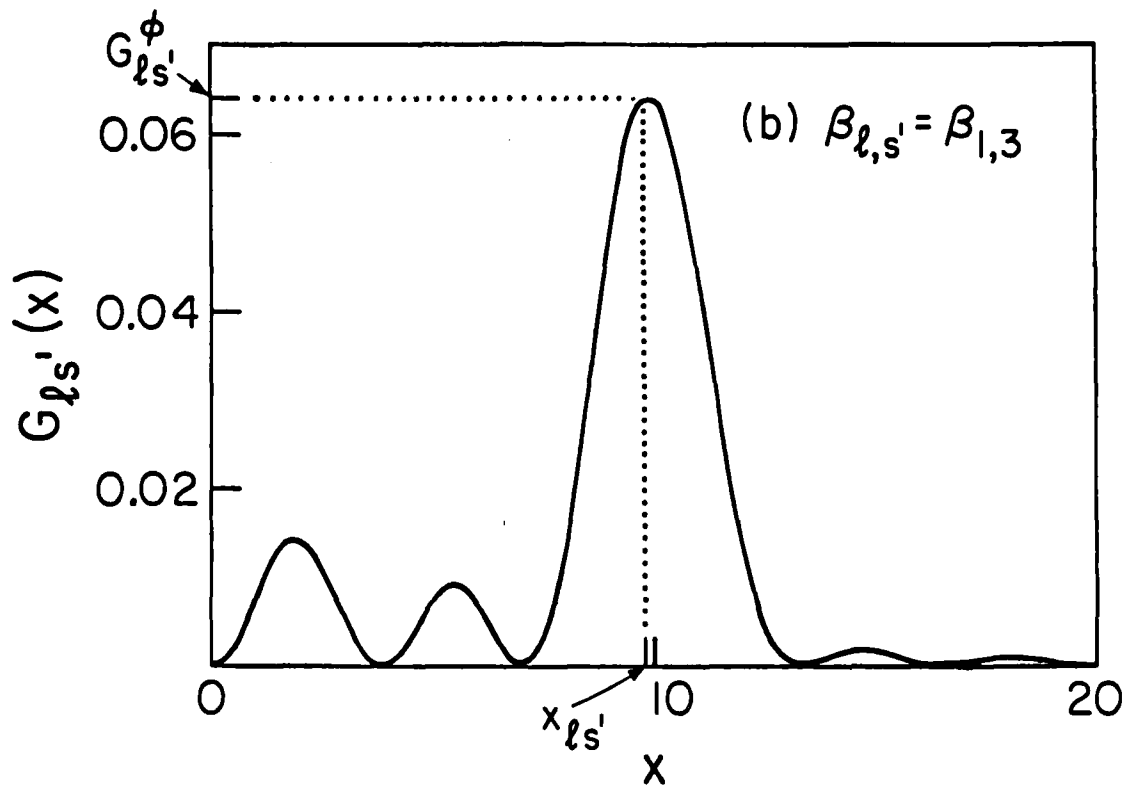


FIGURE 1(b) $\beta_{l,s'} = \beta_{1,3}$

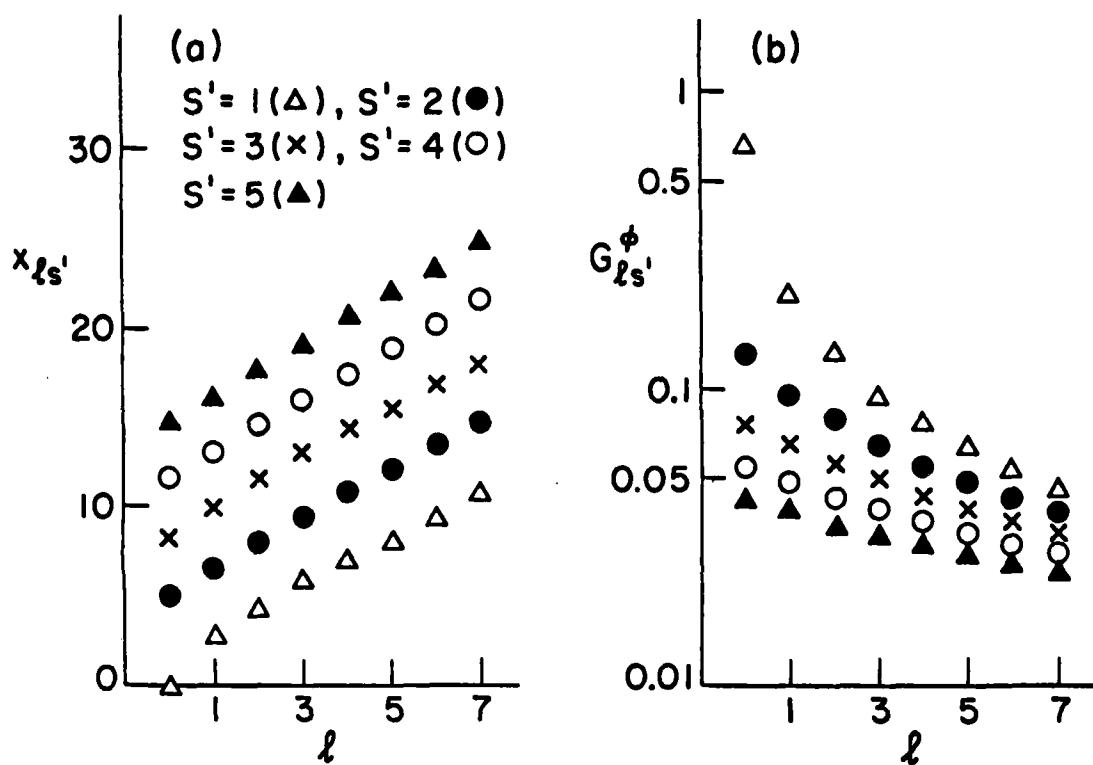


FIGURE 2 PLOTS OF (a) $x_{\ell s'}$ AND (b) THE CORRESPONDING $G_{\ell s'}^{\phi} = G_{\ell s'}(x_{\ell s'})$ FOR SEVERAL VALUES OF AZIMUTHAL AND RAIDAL MODE NUMBERS, ℓ AND s' .

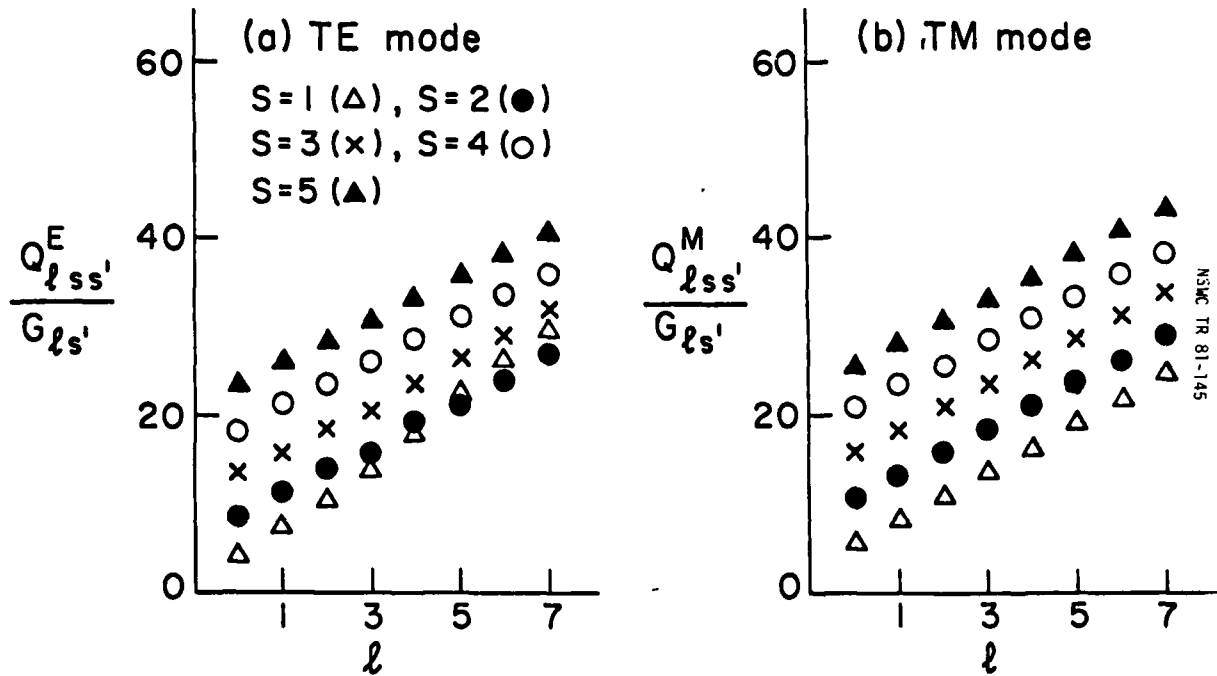


FIGURE 3 PLOTS OF (a) $Q_{lss'}^E/G_{ls'}$ AND (b) $Q_{lss'}^M/G_{ls'}$
EQS. (58) AND (64) FOR SEVERAL VALUES OF l AND s .

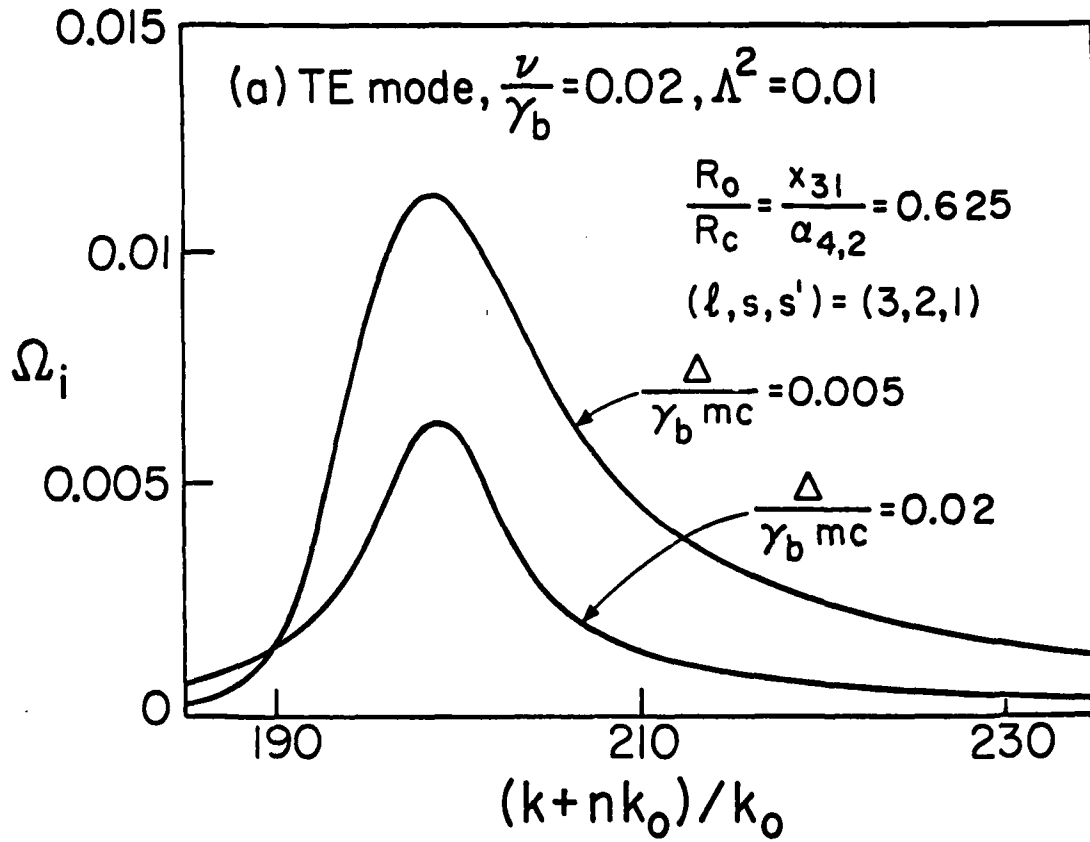
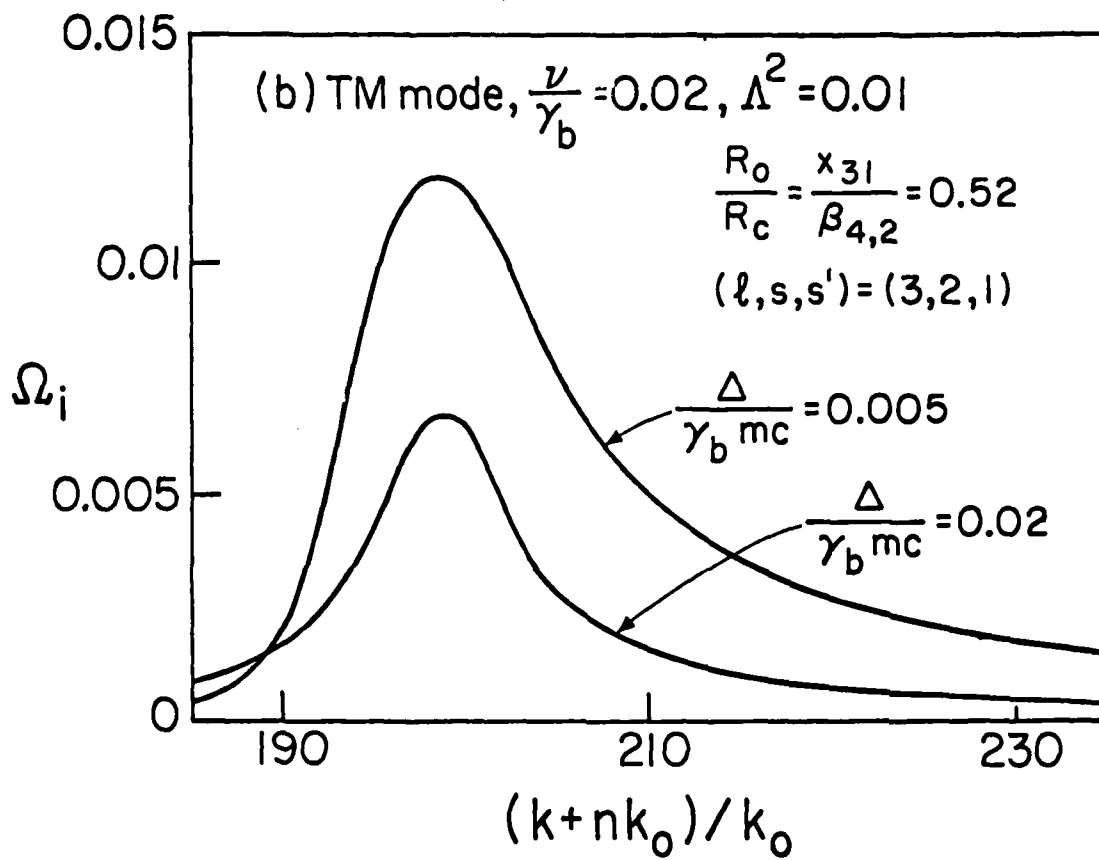


FIGURE 4(a) PLOTS OF NORMALIZED GRWTH RATE Ω_i VERSUS $(k + nk_0)/k_0$ FOR $(l, s, s') = (3, 2, 1)$, $\gamma_b = 10$, $\nu/\gamma_b = 0.02$, AND $\Lambda^2 = 0.01$, WITH (a) $R_0/R_c = x_{31}/a_{4,2}$ FOR THE TE MODE.

FIGURE 4(b) $R_0/R_c = x_{31}/\beta_{4,2}$ FOR THE TM MODE.

BIBLIOGRAPHY

1. T. C. Marshall, S. Talmadge, and P. Efthimion, Appl. Phys. Lett. 31, 320 (1977).
2. D. A. G. Deacon, L. R. Elias, J. M. M. Madey, G. J. Ramian, H. A. Schwettman, and T. I. Smith, Phys. Rev. Lett. 38, 897 (1977).
3. R. C. Davidson and H. S. Uhm, Phys. Fluids 23, 2076 (1980).
4. A. T. Lin and J. M. Dawson, Phys. Fluids 23, 1224 (1980).
5. P. Sprangle, C. M. Tang, and W. M. Manheimer, Phys. Rev. A21, 302 (1980).
6. I. B. Bernstein and J. L. Hirshfield, Phys. Rev. A20, 1661 (1979).
7. H. S. Uhm and R. C. Davidson, "Theory of Free Electron Laser Instability in a Relativistic Annular Electron Beam", submitted for publication (1980).
8. H. S. Uhm and R. C. Davidson, "Free Electron Laser Instability for a Relativistic Annular Electron Beam in a Helical Wiggler Field", submitted for publication (1980).
9. J. R. Bayless, Bull. Am. Phys. Soc. 25, 753 (1980).
10. R. C. Davidson and H. S. Uhm, "Helically Distorted Relativistic Electron Beam Equilibria for Free Electron Laser Applications", submitted for publication (1980).
11. J. D. Jackson, Classical Electrodynamics (John Wiley & Sons, Inc., New York, 1962), Ch. 8.
12. R. C. Davidson, Theory of Nonneutral Plasmas (Benjamin, Reading, Mass., 1974), Ch. 2.

APPENDIX A

LONGITUDINAL PERTURBATIONS FOR THE FREE ELECTRON LASER INSTABILITY

In this Appendix, we investigate properties of the longitudinal perturbations about an electron beam propagating through a cylindrical waveguide with radius R_c . In the present analysis, it is assumed that the perturbations have short wavelength with

$$|q_n^2| = |(k + nk_0)^2 - \omega^2/c^2| \gg 1/R_0^2, \quad (A.1)$$

which can also be expressed as

$$q_n^2 R_0^2 = (1 + v_b/c)^2 \gamma_b^2 k_0^2 R_0^2 \gg 1, \quad (A.2)$$

for the frequencies of interest for free electron laser applications.

Equation (A.2) is easily satisfied in parameter regimes of present experimental interest. In the limit of a small wiggler amplitude ($\Lambda \rightarrow 0$), we obtain the longitudinal eigenvalue equation,

$$\begin{aligned} & \left(\frac{1}{r} \frac{\partial}{\partial r} r \frac{\partial}{\partial r} - \frac{\ell^2}{r^2} - q_n^2 \right) \hat{E}_{z,\ell}^{(n)}(r) \\ & = - \frac{(\omega_{pb}^2/\gamma_b^2) q_n^2 \hat{E}_{z,\ell}^{(n)}(r) \Theta(R_0 - r)}{[\omega - (k + nk_0)v_b + i|k + nk_0|\Delta/\gamma_b^3]^2}, \end{aligned} \quad (A.3)$$

from Eqs. (33), (45), (46), and (56). In Eq. (A.3), $\Theta(x)$ is the Heaviside step function defined in Eq. (52), and $\omega_{pb}^2 = 4vc^2/\gamma_b R_0^2$ is the plasma-frequency-squared.

For notational simplicity, we define

$$\delta\phi^{\ell}(r) \equiv \hat{E}_{z,\ell}^{(n)}(r). \quad (A.4)$$

Inside the electron beam ($0 \leq r < R_0$), Eq. (A.3) can be expressed as¹²

$$\left(\frac{1}{r} \frac{\partial}{\partial r} r \frac{\partial}{\partial r} - \frac{\ell^2}{r^2} + T^2 \right) \delta\phi_{\ell}^{\ell}(r) = 0, \quad 0 \leq r < R_0, \quad (\text{A.5})$$

where

$$T^2 \equiv q_n^2 \left\{ \frac{\omega_{pb}^2 / \gamma_b^2}{[\omega - (k + nk_0)v_b + i|k + nk_0|\Delta/\gamma_b^3]^2} - 1 \right\}. \quad (\text{A.6})$$

Outside the electron beam ($R_0 < r < R_c$), Eq. (A.3) reduces to the free-space eigenvalue equation

$$\left(\frac{1}{r} \frac{\partial}{\partial r} r \frac{\partial}{\partial r} - \frac{\ell^2}{r^2} - q_n^2 \right) \delta\phi_{\ell}^{\ell}(r) = 0, \quad R_0 < r < R_c; \quad (\text{A.7})$$

The solution to Eq. (A.5) that remains finite at $r = 0$ is

$$\delta\phi_{\text{in}}^{\ell}(r) = \hat{\phi}_{\ell} J_{\ell}(TR), \quad 0 \leq r < R_0, \quad (\text{A.8})$$

where $J_{\ell}(x)$ is the Bessel function of the first kind of order ℓ , and $\hat{\phi}_{\ell}$ is a constant. Noting $q_n^2 R_0^2 \gg 1$ in Eq. (A.2), we can express the solution to Eq. (A.7) as

$$\delta\phi_{\text{out}}^{\ell}(r) = C [I_{\ell}(q_n r) K_{\ell}(q_n R_c) - K_{\ell}(q_n r) I_{\ell}(q_n R_c)], \quad R_0 < r \leq R_c, \quad (\text{A.9})$$

where I_{ℓ} and K_{ℓ} are modified Bessel functions of order ℓ , and C is a constant.

The boundary conditions on $\delta\phi_{\ell}^{\ell}(r)$ at the surface of the electron beam are given by

$$[\delta\phi_{\text{in}}^{\ell}]_{r=R_0} = [\delta\phi_{\text{out}}^{\ell}]_{r=R_0}, \quad (\text{A.10})$$

and

$$[\partial/\partial r \delta\phi_{\text{in}}^{\ell}]_{r=R_0} = [(\partial/\partial r) \delta\phi_{\text{out}}^{\ell}]_{r=R_0}, \quad (\text{A.11})$$

from Eq. (A.3). Substituting Eqs. (A.8) and (A.9) into Eqs. (A.10) and (A.11) gives

$$\begin{aligned}
 TR_0 \frac{J'_l(TR_0)}{J_l(TR_0)} &= h(q_n) \\
 &\equiv q_n R_0 \frac{I'_l(q_n R_0) K_l(q_n R_c) - I_l(q_n R_c) K'_l(q_n R_0)}{I_l(q_n R_0) K_l(q_n R_c) - I_l(q_n R_c) K_l(q_n R_0)},
 \end{aligned}
 \tag{A.12}$$

where the "prime" notation denotes derivative with respect to the complete argument of the Bessel function, e.g., $J'_l(TR_0) = [dJ_l(x)/dx]_{x=TR_0}$. The expression for the longitudinal wave admittance $h(q_n)$ in Eq. (A.12) can be simplified in several limiting cases, including short wavelength perturbations with $|q_n^2 R_0^2| \gg 1$. In this case, $h(q_n)$ can be approximated by

$$h(q_n) = -q_n R_0 \coth q_n (R_c - R_0), \tag{A.13}$$

and Eq. (A.12) reduces to

$$-TR_0 \frac{J'_l(TR_0)}{J_l(TR_0)} = q_n R_0 \coth q_n (R_c - R_0). \tag{A.14}$$

Evidently, the right-hand side of Eq. (A.14) is a very large positive number, and the lowest-order longitudinal dispersion relation (for $\Lambda \rightarrow 0$) can be approximated by

$$J_l(TR_0) \approx 0, \tag{A.15}$$

where T is defined in Eq. (A.6). It follows from Eq. (A.15) that

$$T^2 R_0^2 = \beta_{l,s}^2, \quad s' = 1, 2, \dots, \tag{A.16}$$

where $\beta_{l,s'}$ is the s' th zero of $J_l(x) = 0$. In this regard, Eqs. (A.8) and (A.9) can be approximated by

$$\delta\phi^l(r) = \begin{cases} \hat{\phi}_{l,s'} J_l(\beta_{l,s'} r/R_0), & 0 \leq r < R_0, \\ 0, & \text{otherwise,} \end{cases}
 \tag{A.17}$$

where $\hat{\phi}_{l,s'}$ is a constant. Substituting Eq. (A.6) into Eq. (A.16)

and making use of Eq. (A.2), we obtain the longitudinal dispersion relation,

$$\left(\omega - (k + nk_0)v_b + i \frac{|k + nk_0|\Delta}{\gamma_b^3} \right)^2 - \frac{\omega^2}{\gamma_b^2} = 0, \quad (\text{A.18})$$

where the term proportional to $\beta_{l,s}^2$, has been neglected.

DISTRIBUTION

Copies

Naval Research Laboratory
Attn: Dr. M. Lampe
Washington, D.C. 20365

1

Office of Naval Research
Attn: W.J. Condell (ONR-421)
Washington, D.C. 20350

1

U.S. Army Ballistic Research Laboratory
Aberdeen Proving Ground
Attn: Dr. D. Eccleshall (DRDAR-BLB)
Aberdeen, Maryland 21005

1

Air Force Weapons Laboratory
Kirtland Air Force Base
Attn: Maj. H. Dogliana
Albuquerque, New Mexico 87117

1

Department of Energy
Attn: Dr. T. Godlove (C-404)
Washington, D.C. 20545

1

National Bureau of Standards
Attn: Dr. J.M. Leiss
Gaithersburg, Maryland 20760

1

Austin Research Associates, Inc.
Attn: Dr. W.E. Drummond
1901 Rutland Drive
Austin, Texas 78758

1

Ballistic Missile Defense Advanced Technology Center
Attn: Dr. L.J. Harvard (BMDSATC-1)
P.O. Box 1500
Huntsville, Alabama 35807

1

B.K. Dynamics, Inc.
Attn: Dr. R. Linz
15825 Shady Grove Road
Rockville, Maryland 20850

1

DISTRIBUTION (con't.)

	Copies
The Charles Stark Draper Laboratory, Inc. Attn: Dr. E. Olsson 555 Technology Square Cambridge, Massachusetts 02139	1
Director Defense Advance Research Projects Agency Attn: Dr. J. Mangano 1400 Wilson Boulevard Arlington, Virginia 22209	1
IRT Corporation Attn: Mr. W. Selph P.O. Box 81087 San Diego, California 92138	1
Los Alamos Scientific Laboratory Attn: Dr. G. Best P.O. Box 1663 Los Alamos, New Mexico 87545	1
Mission Research Corporation Attn: Dr. C. Longmire 735 State Street Santa Barbara, California 93102	1
Physical Dynamics, Inc. Attn: Dr. K. Breuckner P.O. Box 977 La Jolla, California 92037	1
Sandia Laboratories Attn: Mail Services Section for: Dr. R.B. Miller Albuquerque, New Mexico 87115	1
Science Applications, Inc. Attn: Dr. M.P. Fricke 1200 Prospect Street La Jolla, California 92037	1

DISTRIBUTION (con't.)

	Copies
Science Applications, Inc. Attn: Dr. R. Johnston Dr. J. Siambis 2680 Hanover Street Palo Alto, California 94304	1 1
University of California Lawrence Livermore Laboratory Attn: Dr. R.J. Briggs Dr. E. Lee P.O. Box 808 Livermore, California 94550	1 1
Defense Technical Information Center Cameron Station Alexandria, Virginia 22314	12
Naval Sea Systems Command Washington, D.C. 20362 Attn: SEA-09G32 SEA-03B	2 1

TO AID IN UPDATING THE DISTRIBUTION LIST
FOR NAVAL SURFACE WEAPONS CENTER, WHITE
OAK TECHNICAL REPORTS PLEASE COMPLETE THE
FORM BELOW:

TO ALL HOLDERS OF NSWC/TR 81-145
by Han S. Uhm, Code R41

DO NOT RETURN THIS FORM IF ALL INFORMATION IS CURRENT

A. FACILITY NAME AND ADDRESS (OLD) (Show Zip Code)

NEW ADDRESS (Show Zip Code)

B. ATTENTION LINE ADDRESSES:

C.

☐ REMOVE THIS FACILITY FROM THE DISTRIBUTION LIST FOR TECHNICAL REPORTS ON THIS SUBJECT.

D. NUMBER OF COPIES DESIRED _____

**DEPARTMENT OF THE NAVY
NAVAL SURFACE WEAPONS CENTER
WHITE OAK, SILVER SPRING, MD. 20910**

**OFFICIAL BUSINESS
PENALTY FOR PRIVATE USE, \$300**

**POSTAGE AND FEES PAID
DEPARTMENT OF THE NAVY
DOD 316**



**COMMANDER
NAVAL SURFACE WEAPONS CENTER
WHITE OAK, SILVER SPRING, MARYLAND 20910**

ATTENTION: CODE R41